Remarks

The headings in the Amendment correspond to the headings in the Office Action.

1) As requested, the first line of the specification is amended to read:

--- This application is a 371 of PCT/IB97/01634, filed 10/17/1997. ---

2) Claim 8

a) the term "substitute of the group consisting of" at the top of the second line of the claim is amended to recite standard Markush language, i.e. --- substance selected from the group consisting of ---;

b) the term "bindings" at the fourth line of the claim is amended to read --- binders ---; and

c) the terms "Surfactants" and "Flavours" at the last line of the claim is placed in the lower case.

3) In claim 9, "at least one of the group" is amended to read --- member selected from the group consisting of ---.

Indefiniteness Rejection

Claims 1-3 and 5-11 stand rejected under 35 USC 112(2) as being indefinite.

To point 1) of the Office Action:

According to the Office Action, the claimed "average particle size" values in the claims are stated to be indefinite, as the claimed values are alleged to vary with its method of measurement.

We respectfully disagree.

The size of a HAP particle is an objective value which is inherent to the HAP particle itself and does not depend on the method of measurement.

Furthermore, someone skilled in the art knows which method of measurement can be utilized to determine the size of such HAP particle of a given range of size.

Please find enclosed parts of two scientific articles, explaining the method of measurement for the claimed particle size.

The first article "Two-Dimensional Crystalline Hydroxyapatite" has been written by the inventors of the present invention: Rudin, Komarov, Melikhov, and Bozhevopnov, and by Mr. Severin who is not an inventor.

According to this article, the hydroxyapatite particles were first studied by High-resolution transmission electron microscopy (HRTEM) to obtain electron diffraction patterns. This method is used to determine the length l of the particles (Please note, that the length l as cited in the application is denoted as width l in the article). The determined distribution by length l is shown in Fig. 2 of the article.

The thickness of the HAP particles which are determined to be nanoplates with a HAP crystal lattice determined with a scanning tunneling microscope of type STM NS 100-lv. The evaluated distribution function is shown in Fig. 3.

Both are explained in detail in this article in col. 1, par. 2.

The other article "Electron diffraction from micro- and nanoparticles of hydroxyapatite" by Mrs. Suvorova and Mr Buffat describes the same method of high-resolution transmission electron microscopy (HRTEM), i.e. electron diffraction to examine the hydroxyapatite.

Summarizing, the length of the particles (in the terminology of the application) can be determined by **electron diffraction** (or electron scattering in the terminology of the Examiner) and the thickness by a tunneling microscope.

However, it is not excluded that the particle size can also be determined with other methods.

To point 2) of the Office Action:

Claim 5 is deleted and the term "ultra finely divided" is deleted from claims 6 and 7.

To point 3) of the Office Action:

We agree with the amendments of claims 6 and 8 as proposed by the Examiner.

The last line of claim 6 is amended to read --- 50% by weight, based on the weight of the stomatic composition ---.

To points 4), 5) and 6) of the Office Action:

We agree with the proposals of the Examiner.

Claim 9, second line, is changed from "the gingivitis system of the mouth cavity" to gingivitis treatment agents". The term "gigivitits system" at claim 11, line 4 is changed similarly.

Claim 9, fourth line, the open-ended term "etc." is deleted.

Claim 9, last line, "the aqueous" and "the aqueous-alcoholic" are changed to "an aqueous" and "an aqueous-alcoholic", as is done in claim 11.

A Terminal Disclaimer is submitted herewith.

A three-month extension of time in which to respond to the outstanding Office Action is hereby requested. PTO-2038 authorizing credit card payment for the amount of $490 is enclosed for the prescribed Small Entity three-month extension fee.

In addition, the prescribed Small Entity Statutory Disclaimer fee of $55 is included with the extension fee.

Respectfully submitted,

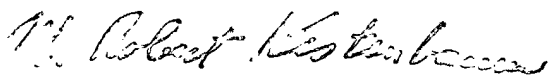

M. Robert Kestenbaum
Reg. No. 20,430
11011 Bermuda Dunes NE
Albuquerque, NM USA 87111
Telephone (505) 323-0771
Facsimile (505) 323-0865

CERTIFICATE OF MAILING BY FIRST CLASS MAIL

I hereby certify under 37 CFR §1.8(a) that this correspondence is being deposited with the United States Postal Service as first class mail with sufficient postage on the date indicated below and is addressed to the Commissioner for Patents, P.O. Box 1450, Alexandria, VA 22313-1450 on November 2, 2004.

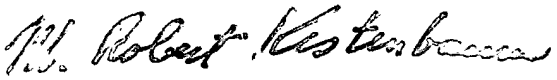

M. Robert Kestenbaum

Volume 373, Numbers 1 – 3
July 2000

ISSN: 0012-5016
CODEN: DKPCAG

DOIKLADY PHYSICAL CHENISTRY

Enhlish Translation of *Doklady Akademii Nauk*
(vol.373, Nos. 1 – 3, July 2000)

Editor-in-Chief
Viktor A.Kabanov

Translated and Published by

МАИК "НАУКА/INTERPERIODICA" PUBLISHING

Distributed worldwide by KLUWER ACADEMIC/PLENUM PUBLISHERS

Two-Dimensional Crystalline Hydroxyapatite

Corresponding member of the RAS I. V. Melikhov*, V. F. Komarov*, A. V. Severin*, V. E. BozhevoPnov*, and V. N. Rudin**

Received February 8, 2000

Hydroxyapatite $Ca_{10}(PO_4)_6(OH)_2$ (HAP) is one of few biocompatible mineral substances. This motivates a sustained interest to synthesis and properties of this compound. Diverse procedures for synthesis of HAP crystals of various habit and size were developed [1-3]. However, the potentialities of synthesis of new forms are not exhausted. In this work, HAP in a two-dimensional crystalline form was obtained by rapid mixing of reagent solutions under certain temperature and hydro-dynamic conditions.

Fig. 1 presents TEM images of grains of the solid phase obtained by a short-term feeding of an H_3PO_4 solution stream into a reaction vessel filled with a 0.02 M $Ca(OH)_2$ solution thermostatically controlled (298 K) and vigorously stirred. The atomic calcium : phosphorus ratio was 1.67 ± 0.01. The resulting mixture was stirred at 298 K. Solid particles were sampled from the reaction vessel at various intervals t after feeding the acid and dried by sublimation. Since the phase obtained was amorphous (as probed by X-ray powder diffraction; DRON diffractometer, CuK_a radiation), the samples were studied further by transmission electron microscopy. High-resolution TEM images of grains were obtained on an SM 300 microscope with a field-ion electron source [4]. The images were analyzed using the Digital Micrograph program and compared with the images calculated with the use of the EMS program [5]. We found that, at $t = 10^4$ s, all particles were nanoplates with a HAP crystal lattice. Each discrete particle gave a point electron diffraction pattern. Electron diffraction images of aggregates were diffuse, with two wide rings. The plate distribution by width / is shown in Fig. 2. The thickness of nanoplates h was determined on an STM NS 100-lv tunneling microscope (Moscow, Institute of Nanotechnologies)*. The determinations were precise enough to evaluate the distribution function $\psi(h, t)$ by h (Fig. 3).

According to the chemical analysis data, the composition of the phase after drying in air at 293 K to constant weight was

$$Ca_{10}(PO_4)_6(OH)_2 \cdot 3H_2O \quad (1)$$

A reversible dehydration of this phase occurs at 400K. Phase analysis carried out with the use of electron diffraction and TEM images (including calculated images) unambiguously shows that the phase has the structure of hydroxyapatite. Therefore, water molecules present in the compound of formula (1) do not enter in the crystal lattice of HAP, but are chemisorbed on nanoplates, which have a large surface area.

Since the thickness of nanoplates is equal to 1-3 unit cell parameters, the compound synthesized may be called two-dimensional crystalline pseudo crystal hydrate with a HAP structure or two-dimensional crystalline hydroxyapatite (TDHAP).

Our studies showed that the following processes take place in the reaction vessel in the course of synthesis of TDHAP. Immediately after addition of the acid, nanoplates of the $Ca_8H_2(PO_4)_6$ composition with the structure of octacalcium phosphate (OCP) appear in the solution. The plate sizes are shown in Figs. 2 and 3. This composition of the plates was derived from the changes in the calcium and phosphorus amounts and in the pH values of the solution in the time interval t = $10\text{-}10^2$ s. We failed to determine whether or not these nanoplates contained chemisorbed water, since they change their composition when removed from the reaction vessel. In the runs described, a suspension sample containing nanoplates was removed from the reaction vessel and was slowly dried or rapidly frozen. The ice formed was then sublimated. Upon water evaporation or ice formation, a fraction of nanoplates was converted into TDHAP. The remaining nanoplates (of the OCP composition) were unstable in an electron beam of the microscope. However, we succeeded in identifying some of them by their electron diffraction patterns and demonstrated that they had the structure of OCR Taking into account that nanoplates are converted into TDHAP, we assume that they contain a large amount of chemisorbed water; i.e., the first product of the synthesis is the two-dimensional crystalline octacalcium phosphate.

The OCP nanoplates sorb $Ca(OH)_2$ from the solution. which is accompanied by the reaction

$$Ca_8H_2(PO_4)_6 + 2Ca(OH)_2 \rightarrow Ca_{10}(PO_4)_6(OH)_2 + 2H_2O. \quad (2)$$

* *Moscow Stale University Vorob'evy gorv. Moscow, 119899 Russia*

** *Samoilov Institute of Pert Hirers. Insecticides, and Fungicides. Leninskii pr. 55, Moscow, 117917 Russia*

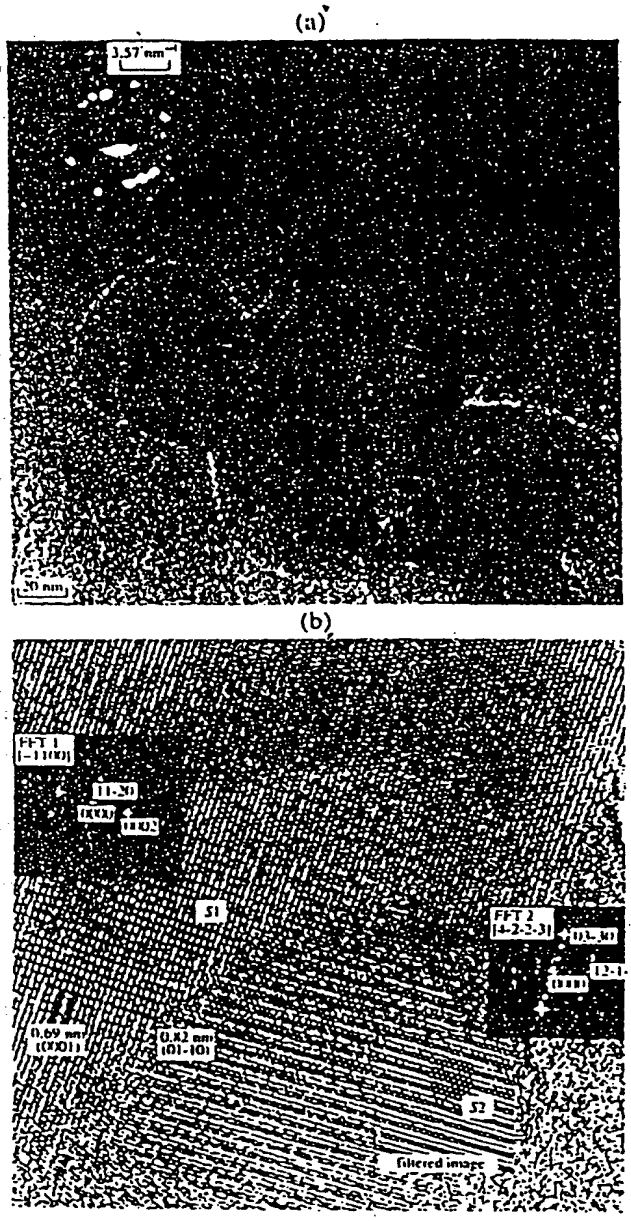

Fig. 1. HREM images of typical TDHAP nanoplates at (a) $t = 10$ s and (b) $t = 40$ s. Filtered imageS (S1) along the [1100] direction at a tentative thickness of 3.3 nm and a defocussing of 30 nm and (52) along the [4223] direction at a tentative thickness of 2.0 nm and a defocussing of 33 nm.

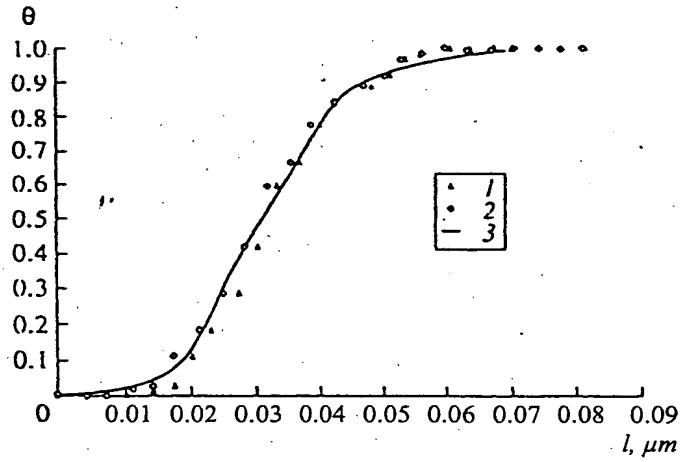

Fig. 2. Integral function of nanoplate distribution by width (0 denotes the fraction of nanoplates with a width lesser than l) at sampling at (t) $t = 10^2$ s (drying by sublimation). (2) $t = 10^4$ s (filtration through a tracking filler, drying in air), and (3) calculation according to the model (3)-(6) at $x_1 = x_2 = l$, $m_0 = m_1 = m_2, \xi_0 > 10^3$, $h_0 \Omega_{10} C_0 (Jp) = 38.98$ nm^2 . (ρ is the crystal density), and $f_{10}/\Omega_{10} = 5.3 \times 10^3$ nm^3.

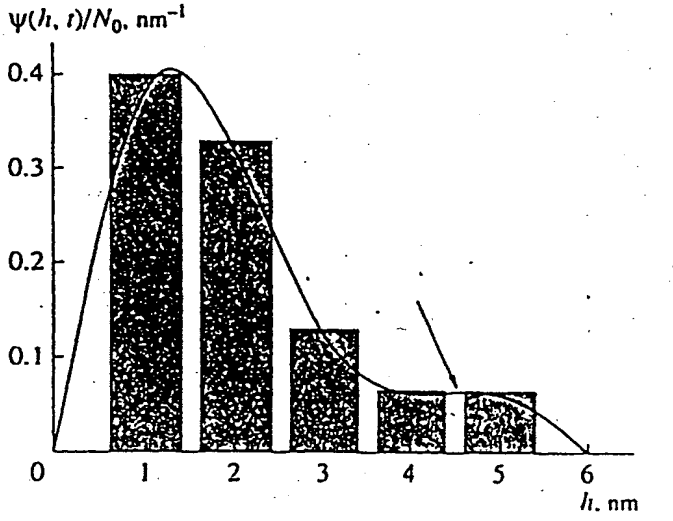

Fig. 3. Function of nanoplate distribution by width after drying by sublimation ($t = 10$ s). The region, where the influence of aggregation is exhibited, is marked by the arrow.

Reaction (2) proceeds without breaking nanoplates and almost without changing their sizes: crystal nuclei of HAP appear in each nanoplate, relatively rapidly grow throughout the volume, and can go to neighboring plates. The HAP nuclei are formed at various times so that the amount of nanoplates converted into TDHAP increases with time, as is shown in Fig. 4. At $t \rightarrow 10^4$ s, nearly all nanoplates are converted into HAP and process (2) is completed. Further, plates become thicker and more perfect in shape. As the plates are thickened, X-ray diffraction patterns of the solids removed from the reaction vessel change from a pattern typical of amorphous substances to a pattern characteristic of three-dimensional HAP. A thickening of the plates becomes noticeable at $t > 10^5$ s. In the time range of $t = 20\text{-}10^5$ s, the size and the shape of the plates remain vir-

unaltered. Therefore, TDHAP is formed from the OCP precursor and inherits its two-dimensional crystalline state, which is turned to be rather stable in an aqueous solution.

The reasons for the relative stability of OCP and TDHAP can be established using the following model.

At $t = 0 - 10^2$ s, the function of distribution $\varphi(x_i, t) = \frac{\partial^3 N}{\partial x_1 \partial x_2 \partial x_3}$ of OCP crystals by size $\{x_i\}$ changes according to the Fokker-Planck equation in the form

$$\frac{\partial \varphi}{\partial t} = \sum_{i=1}^{3} \frac{\partial}{\partial x_i}\left[\frac{\partial}{\partial x_i}(D_i\varphi) - G_i\varphi\right] - W_\varphi \qquad (3)$$

at $\varphi(x_i,0) = \varphi(\infty,t) = 0$ and

$$\int_0^\infty\int_0^\infty \left\{G_1\varphi - \frac{\partial}{\partial x_i}(D_1\varphi)\right\}_{x_1\to 0} dx_2 dx_3 = J(\xi^{m_0} - 1), \qquad (4)$$

where N is the concentration of crystals whose dimensions are smaller than $\{x_i\}$; G_i and D_i, are the rate of the directed change in x_i and the rate fluctuation coefficient, respectively; W denotes the rate of crystal aggregation; J is the characteristic nucleation rate; $\xi = C/C_\infty, C$ and C_∞ are the total concentrations of all phosphorus forms in the saturated and supersaturated solutions; and m_0 denotes the order of the nucleation reaction.

In crystal growth, ion clusters are formed at the surface of each crystal face at a rate Ω_i. These clusters contain one or several PO_4 groups. These clusters grow across the face at the rate f_i, thus forming a new layer of the solid substance. According to [6],

$$G_i = h_0\Omega_i S_i / P, \quad D_i = (1/2)\Omega_i S_i (h_0/P)^2, \qquad (5)$$

where S_i is the face surface area; h_0 is the thickness of a layer; h_0/P denotes the average increment in x_i as a result of the formation and growth of one cluster; and

$P = 1 + S_i(\Omega_i / f_i)^{2/3}$ according to [7], and

$$\Omega_i = \Omega_{i0}[\xi^{m1} - \xi_n^{m1}], \quad f_1 = f_{i0}[\xi^{m2} - \xi_n^{m2}]. \qquad (6)$$

Here, Ω_{i0} and f_{i0} represent the characteristic values of Ω_i and f_i, respectively; m_1 and m_2 are the orders of the reactions of formation and growth of clusters; $\xi_n = C_n/C_\infty$ and C_n denotes the solubility of the crystal, determined by the Gibbs-Thomson formula with the Tolmen correction factor.

Let us assume that the rate Ω_i is so high for some faces that $P = S_i(\Omega_i / f_i)^{2/3}$ and so small for other faces that $P = 1$. As this takes place,

$$\Omega_{10}^{1/3} f_{10}^{2/3/} \xi_0^{(2/3)(m_2-m_1)} / (\Omega_{20} b^2) \geq 10^6, \qquad (7)$$

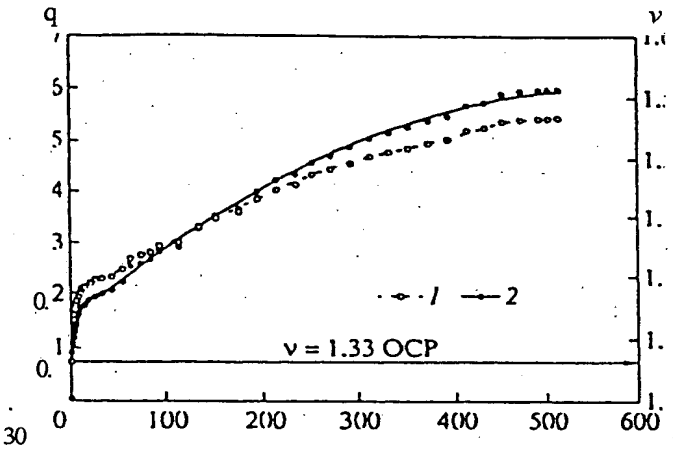

Fig. 4. Properties of the solid phase vs. time: (1) the Ca : P molar ratio (v) and (2) the fraction of nanoplalcs converted from OCP into TDHAP *(q)*.

where b is the unit cell parameter along the perpendicular to the face with the small value of Ω_i, $\xi_0 = C_0/C_\infty$ and Co denotes the initial concentration of the solution.

In this case, as calculations have shown, each crystal is converted immediately after nucleation into a plate whose bases are molecularly smooth faces and the sides are molecularly rough surfaces, as in Fig. 1. The bases of the plates grow so slowly and the side surfaces grow so fast that the plates increase in size almost without thickening. The growth of these plates leads to a decrease in C to the C_n value during a time interval on the order of

$$\tau = 10^2 b / \left[h_0 \Omega_{10}^{1/3} f_{10}^{2/3} \xi_0^{(m_1+2m_2)/3}\right]. \qquad (8)$$

Over this period of time, each plate has managed to grow to $x_1 = l > 10^2 b$ and to thicken only to $x_2 = h \sim b$. Further, the plate sizes change relatively slow because of recrystallization leading to a decrease in concentration C from C_n to C_∞, and because of aggregation occurring at a small rate W.

As a result, at the instant $t \to \tau$ the distributions

$$\theta = (1/N_0)\int_0^{x_1} dx_1 \int_0^\infty dx_2 \int_0^\infty \varphi(x_i,t)dx_3$$

(where N_0 is the concentration of nanoplates) and

$$\psi(h,t) = \int_0^\infty\int_0^\infty \varphi(x_i,t)dx_1 \ldots dx_3$$

take the form observed in our experiments.

We found that numerically solving Eqs. (3)-(7) by the methods [8, 9] at $W = 0$ and adjusting the parameters J, Ω_{i0}, h_0 and f_{i0} led to a good fit of the calculation to the experiment, as is shown in Fig. 2.

Agreement between the calculation and the experiment indicates that the origin of appearing nanoplates

is a sharp anisotropy of the growth of different faces of the OCP crystals. The formation of surface clusters on the-base faces blocked with chemisorbed water occurs more rarely than on the side faces by five orders of magnitude. Because of this, the crystals grow almost without thickening. The C value during this process decreases to the C_n value, at which the bases .of the plates lose a possibility to grow at all because'of an enhanced solubility of crystals. As a result of the fulfillment of the condition $C \rightarrow C_n$, nanoplates become metastable, since they may thicken at $t > 10^2$ s only at the expense of recrystallization or aggregation, which proceed slowly.

The data obtained allow us to assume that calcium phosphates can exist in a limiting two-dimensional crystalline state, in which all crystals are of $h = b$ in thickness at $l > b$.

The TDHAP obtained by us ($b = 0.82$ nm) is not in the limiting state due to adhesion of nanoplates by their faces. The importance of adhesion is confirmed by the fact that the OCP and TDHAP properties depend on the presence of collagen in the reaction vessel. We established that if tropocollagen ($M = 5 \times 10^3$) is introduced into the reaction vessel together with the $Ca(OH)_2$ solution. the specific surface area of nanoplates can be 'determined *in situ* based on the amount of collagen removed with the solid phase from the reactor. Under the given conditions, at $t = 40$ s, the specific surface area was 900 ± 50 m^2 g^{-1}. This value is close to the value 920 ± 20 m^2 g^{-1}, which was calculated on the assumption of the same thickness ($h = b$) for all nanoplates with the size distribution shown in Fig. 2. This means that OCP immediately after the formation was in the limiting two-dimensional crystalline state stabilized with collagen.

Based on these findings, we developed the technology for synthesis of TDHAP [10]. The compound showed itself as an highly efficient medicine, stimulating osteogenesis upon implantation into damages of bone tissues of living organisms [11].

ACKNOWLEDGMENTS

This work was supported by the Russian Foundation for Baste Research, project no. 97-03-32976. and by the Program "Universities of Russia" (project no. 5053). Electron microscopic studies were performed at CIME-EPFL (Lausanne) and supported by Oerlikon Contravcs AG, and the studies on a tunneling microscope were carried out at the Institute of Nanotechnologies (Moscow). We thank E.I. Suvorova for her help with high-resolution electron microscopy.

REFERENCES

1. Dricssens, F.C.M. and Verbceck, R.M.H., *Biominerals,* Boston: CRC Press. 1990.
2. Tsuda, H. and Arends, J.. J. *Dent. Res.,* 1994. vol. 204, p.1050.
3. Suvorova. E.I., Christensson. F. Landager Madsen. M.E./ and Chcrnov.A.A.,.7. Cror. *Crowds* 1998, vol. 186, no. 1, p.262.
4. Suvorova, E.I., Polyak. L.E.. Komarov. V.F., and Melikhov. LV., *KristaHografiya,* 2000. vol. 45, no. 4. p. 40.
5. Stadelmann. P.A.. *Ultramicroscop*\\ 1987. vol. 21. no. 1. p. 131.
6. Mdikhov. I.V.. Z/i. *F^. Khim.,* 1989. vol. 63. no. 2. p. 476.
7. Obrctenov. W. and Bostanov. V.. *J. Crvst. Growth,* 1992. vol. 121. p. 495. '
8. Berliner, L.B. and Melikhov, I.V., *Teoi: Osn. Khim. Tekh-noL,* 1985, vol. 19. no. I. p. 24.
9. Samarskii. A.A. and Vabishevich. P.N.. *Computational Heat Transfer,* Chichester: Wiley, 1995. vols. 1.2.
10. Patent PCT/IB97/01414.'
11. Patent ER 0664 133.

Journal of Microscopy, Vol. 196 Pt 1, October 1999, pp. 46–58.
Received 12 April 1999; accepted 10 May 1999

Electron diffraction from micro- and nanoparticles of hydroxyapatite

E. I SUVOROVA* [1] & P. A. BUFFAT I
* *Institute of Crystallography Leninsky pr.*, 59 Moscow 117333 *Russia*
ı *Centre Interdepartemental de Microscopie Electronique, Ecole Polytechnique Federale de Lausanne. 1015 Lausanne Switzerland*

Key words. Bones, electron diffraction, high-resolution electron microscopy, hydroxyapatite, image processing, image simulation, micro- and nanoparticles.

Summary

Hydroxyapatite (HAP) obtained from aqueous solutions under different conditions has been examined by high-resolution transmission electron microscopy (HRTEM) and electron diffraction, including selected-area electron diffraction (SAED) and microdiffraction A Philips CM300 field-emission gun electron microscope with a Schottky W/ZrO field-emission tip and a spherical aberration constant of 0.65 mm was used at 300 kV. The HAP crystals had different sizes, ranging from a few nanometres to a few micrometres. Single-crystal diffraction patterns have been obtained from the largest microcrystals using the conventional SAED technique. Assemblies of nanoparticles gave only broad diffuse rings. Nevertheless, microdiffraction with electron microprobes 3.5-10nm in diameter clearly indicated the crystalline character of the nanoparticles in these assemblies. Experimental HRTEM images. Fourier transforms and calculated images exhibited the fine structure of the HAP crystals.

Introduction

Recent developments of methods and instruments for structural investigation of solids open a way to receive reliable data from small areas in samples and submicrometresized particles concerning their phase composition, morphology and crystal structure. The combination of high-resolution transmission electron microscopy (HRTEM), including image calculation and image processing, selected-area and nanoprobe electron diffraction allowed us to observe morphology and structure of micro- and nanoparticles of hydroxyapatite (HAP) and to prove their crystalline character.

Correspondence to: Philippe A. Buffat. Tel: + 41 21693 2983/4405; tax:+ 41 21 693 4401; e-mail: philippe.buffat@epfl.ch
Presently at Centre Interdepartemental de Microscopie Electronique, EPFL. 1015 Lausanne E-mail: elena.suvororova@epfl.ch

The knowledge of hydroxyapatite microstructure is important on several accounts First it is a component of bones, and the study of nucleation and growth of the HAP crystals in aqueous solutions under conditions close to biological environment (T = 37°C pH 7.4, dilute solutions) gives us the possibility to model the processes of biomineralization and demineralization, that is, formation and destruction of bone tissue Second it is also a biocompatible implant for a bone tissue. The determination of the correlation between morphology and structure of the HAP particles on the one hand and growth conditions on the other hand allows us to choose the requisite temperature. concentrations and pH of the initial reagents for direct and rational synthesis of the pure substance with definite and optimal morphology and size of particles

Hydroxyapatite. Ca_{10} $(OH)_2(P0_4)_6$, has a hexagonal unit cell with $P6_3/m$ space group and parameters a = 0.942 and c = 0.688 nm (Kay *et al.*, 1964). As a rule, the HAP crystals are thin anisotropic platelets elongated in the c direction, which is the predominant direction of growth. The length of the HAP crystals obtained from aqueous solutions under terrestrial conditions lie within a wide range, from a few nanometres to a few micrometres, while under microgravity conditions they are at least 1.5 orders of magnitude larger than the largest crystals on earth (Lundager Madsen *et al.*, 1995). It was suggested that the increase in the HAP crystal size occurs as a result of lower supersaturation in the crystallization system because of the absence of convection in space and the strong reduction in the rate of nucleation. Even if the same initial reagents are used the change of local supersaturation can result in a change of phase composition and sizes (Lundager Madsen *et al.*, 1995. Suvorova *et al.*, 1998).

In this paper we do not give a detailed review of the growth of HAP crystals as this material has already been widely studied. We report our investigation with HRTEM

© 1999 The Royal Microscopical Society

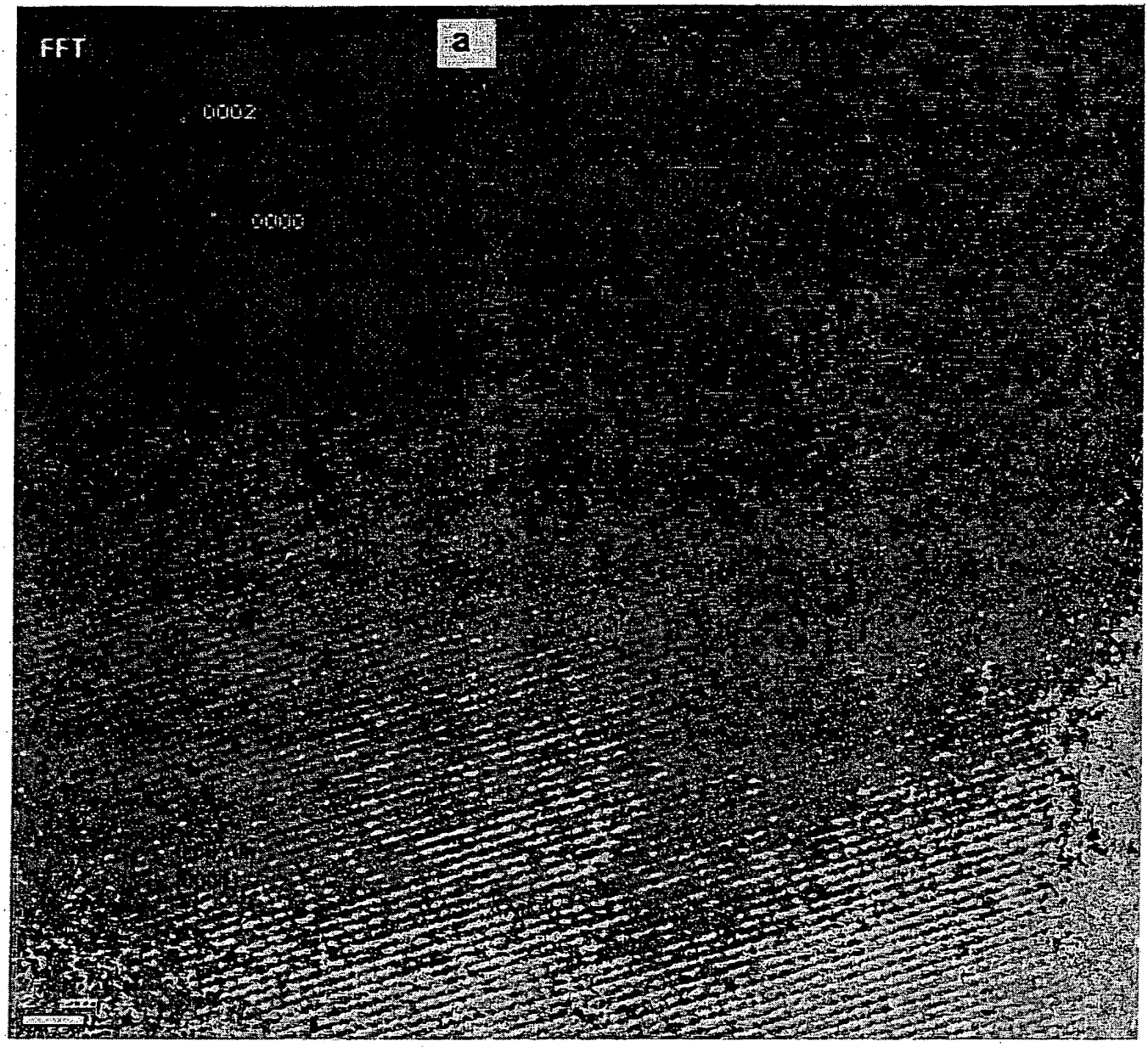

Fig. 8. HRTEM image of a HAP nanoparticle with predominant (0001) fringes and corresponding Fourier transform (a), HRTEM image and Fourier transform obtained normal to the [5410] zone axis (b). The calculated image for 2.5-nm thickness at 33 nm of defocus is inserted in the filtered image.

As mentioned above, prolonged electron irradiation changes the morphology of these nanoparticles. However, we have also shown in a previous experiment (Suvorova *et al.*, 1998) that the HAP structure is quite stable under the electron beam even at higher intensity and examination time compared to the present conditions. Obviously, electron irradiation is unable to crystallise a complex structure such as the HAP structure. Thus, irradiation can only participate in the reorganization or sintering of pre-existing HAP nanoparticles.

The origin of the apparent contradiction between the 'amorphous'-like SAED patterns on agglomerates and the crystalline nature revealed by the microdiffraction and the HRTEM images on thin areas has not yet been entirely elucidated. The fit of HRTEM image simulation to experimental images shows that the nanoparticles are platelets of

This Page is Inserted by IFW Indexing and Scanning Operations and is not part of the Official Record

BEST AVAILABLE IMAGES

Defective images within this document are accurate representations of the original documents submitted by the applicant.

Defects in the images include but are not limited to the items checked:

- ☐ BLACK BORDERS
- ☐ IMAGE CUT OFF AT TOP, BOTTOM OR SIDES
- ☐ FADED TEXT OR DRAWING
- ☐ BLURRED OR ILLEGIBLE TEXT OR DRAWING
- ☐ SKEWED/SLANTED IMAGES
- ☑ COLOR OR BLACK AND WHITE PHOTOGRAPHS
- ☐ GRAY SCALE DOCUMENTS
- ☐ LINES OR MARKS ON ORIGINAL DOCUMENT
- ☐ REFERENCE(S) OR EXHIBIT(S) SUBMITTED ARE POOR QUALITY
- ☐ OTHER: _____

IMAGES ARE BEST AVAILABLE COPY.
As rescanning these documents will not correct the image problems checked, please do not report these problems to the IFW Image Problem Mailbox.